

See discussions, stats, and author profiles for this publication at:  
<https://www.researchgate.net/publication/232392040>

# Temperature dependence of the hyperfine coupling constant of the D<sub>3</sub>O radical: A direct ab initio molecular dynamics (MD) study

ARTICLE *in* CHEMICAL PHYSICS · FEBRUARY 2002

Impact Factor: 1.65 · DOI: 10.1016/S0301-0104(01)00603-6

---

CITATION

1

---

READS

8

## 1 AUTHOR:



[Hiroto Tachikawa](#)

Hokkaido University

285 PUBLICATIONS 2,985 CITATIONS

SEE PROFILE

# Temperature dependence of the hyperfine coupling constant of the $D_3O$ radical: a direct ab initio molecular dynamics (MD) study

Hiroto Tachikawa\*

*Division of Molecular Chemistry, Graduate School of Engineering, Hokkaido University, Kita-ku Sapporo 060-8628, Japan*

Received 13 September 2001

## Abstract

Temperature dependence of hyperfine coupling constants (hfcc's) of the  $D_3O$  and  $H_3O$  radicals, which are the important intermediates in interstellar molecular clouds, has been investigated by means of direct ab initio molecular dynamics (MD) method. The umbrella-bending mode of the  $D_3O$  radical was activated by thermal energy, although the bending structure of the  $D_3O$  radical did not inverse even at 300 K. From the MD calculations, it was predicted that deuterium- and hydrogen-hfcc (D- and H-hfcc) of  $D_3O$  ( $H_3O$ ) increases with increasing temperature, whereas oxygen-hfcc decreases as temperature is increased. The effect of thermal activation on structure and electronic states of  $D_3O$  ( $H_3O$ ) was discussed on the basis of theoretical results. © 2002 Elsevier Science B.V. All rights reserved.

## 1. Introduction

Hydronium radical  $H_3O$  is one of the important species in interstellar molecular clouds for the formation of water molecule which is expressed by  $H_3O^+ + e^- \rightarrow [H_3O] \rightarrow H_2O + H$  [1,2]. The lifetime of  $D_3O$  in gas phase, formed by the charge transfer reaction  $D_3O^+ + Na \rightarrow Na^+ + D_3O$ , is estimated to be the order of microsecond time scale [3–5].

On the other hand, the stability of  $H_3O$  ( $D_3O$ ) in condensed phase has been devoted in the subject of experimental and theoretical investigations for more than 30 years [6]. Martin and Swift [7] ob-

tained further proof about  $H_3O$  in 1971. They measured electron paramagnetic resonance (EPR) spectrum of UV-irradiated perchloric acid glass at 77 K showing quartet EPR lines with isotropic hydrogen hyperfine coupling constant (H-hfcc) of  $H_3O$  of 22.84 G, which is slightly smaller than that of methyl radical  $CH_3$  (23.04 G). They also reported that hfcc of deuterium of  $D_3O$  is 3.65 G and assigned the EPR spectrum of the UV-irradiated perchloric glass to the  $H_3O$  radical. However, Wargon and Williams [8] were not able to reproduce the quartet EPR lines for  $H_3O$  under the conditions reported by Martine and Swift [7]. Node et al. [9] reported that the existence of  $H_3O$  has not yet been experimentally demonstrated. They pointed out that the EPR spectrum of the UV-irradiated perchloric acid glass is significantly close to that of  $CH_3$ , so that to distinguish between

\* Fax: +81-11706-7897.

E-mail address: hiroto@eng.hokudai.ac.jp (H. Tachikawa).

them only from the measurement of hfcc's is quite difficult. Simons and co-workers [10] also pointed out that  $\text{H}_3\text{O}$  is composed of highly distorted radical expressed by  $\text{H}_2\text{O}-\text{H}$  on the basis of their EPR experiment. Thus, the existence of  $\text{H}_3\text{O}$  has been questioned from experimental point of view.

Theoretical works have been carried out for the  $\text{H}_3\text{O}$  system and the dissociative recombination of  $\text{H}_3\text{O}^+$  with electron [11–14]. Ketvirtis and Simons [14] calculated the potential energy (PE) diagram for the  $\text{H}_3\text{O}^+/\text{H}_3\text{O}$  system. They suggested that ground state  $\text{H}_3\text{O}$ , produced by dissociative recombination of  $\text{H}_3\text{O}^+ + \text{e}^-$  at low relative beam energies, can dissociate via several pathways to form  $\text{H}_2\text{O}$  ( $\text{X}^1\text{A}_1$ ) +  $\text{H}$ ,  $\text{OH}$  ( $\text{X}^2\Sigma$ ) +  $\text{H}_2$ , or  $\text{OH}$  ( $\text{X}^2\Sigma$ ) +  $\text{H} + \text{H}$ . The first and second products are exothermic relative to  $\text{H}_3\text{O}$ , whereas the other channels are endothermic. Also, their calculations imply that channel 1 is main channel if excess energy of  $\text{H}_3\text{O}$  is small, although very small activation barrier (the barrier height was calculated by 1.4 kJ/mol) is located between  $\text{H}_3\text{O}$  and the dissociation product ( $\text{H}_2\text{O} + \text{H}$ ).

In a previous paper, we calculated H-hfcc's of  $\text{H}_3\text{O}$  by means of higher-level ab initio molecular orbital (MO) calculations [15]. It was predicted that H-hfcc of  $\text{H}_3\text{O}$  is positive and the magnitude of H-hfcc of  $\text{H}_3\text{O}$  is smaller than that of  $\text{CH}_3$ . These results indicate strongly that double resonance spectroscopy is distinguishable the spectrum of  $\text{H}_3\text{O}$  from that of  $\text{CH}_3$ . However, the hfcc's of  $\text{H}_3\text{O}$  calculated by us are values at 0 K (i.e., without temperature). In order to detect the  $\text{H}_3\text{O}$  and  $\text{D}_3\text{O}$  radicals experimentally, studying on temperature dependence of H-hfcc of  $\text{H}_3\text{O}$  ( $\text{D}_3\text{O}$ ) provides important information about spectroscopic and magnetic properties of  $\text{H}_3\text{O}$  ( $\text{D}_3\text{O}$ ).

In the present study, temperature effect on the H-hfcc of  $\text{H}_3\text{O}$  ( $\text{D}_3\text{O}$ ) is investigated by means of full dimensional direct ab initio molecular dynamics (MD) method in order to support detection of  $\text{H}_3\text{O}$  ( $\text{D}_3\text{O}$ ) in condensed phase.

## 2. Computational methods

In general, the classical trajectory is performed on an analytically fitted PE surface. However, it is

not appropriate to predetermine the reaction surfaces of the present systems because of the large number of degrees of freedom ( $3N - 6 = 6$ , where  $N$  is number of atoms in the system). Therefore, in the present study, we applied the direct ab initio MD calculation with all degrees of freedom to the  $\text{H}_3\text{O}$  and  $\text{D}_3\text{O}$  systems. The detail of direct ab initio MD method is described elsewhere [16–18].

The direct ab initio MD calculations were carried out at the HF/6-311G(d,p) level of theory. The optimized structure of  $\text{H}_3\text{O}$  was used as an initial structure at the MD calculation. We choose four temperatures for simulation ones, 50, 100, 200, and 300 K. Temperature of the systems ( $\text{H}_3\text{O}$  and  $\text{D}_3\text{O}$ ) is defined by

$$T = \frac{1}{3kN} \langle m_i v_i^2 \rangle,$$

where  $N$  is number of atoms,  $v_i$  and  $m_i$  are velocity and mass of  $i$ th atom, and  $k$  is Boltzmann's constant. The PE (total energy) and energy gradient were calculated at each time step. In order to keep a constant temperature of the system, bath relaxation time ( $\tau = 0.01$  ps) was introduced in the MD calculation [2,9–11]. In the MD calculations, we assumed that each atom moves as a classical particle on the HF/6-311G(d,p) multidimensional PE surface. The equations of motion for  $n$ th atoms in a molecule are given by

$$\frac{dQ_j}{dt} = \frac{\partial H}{\partial P_j},$$

$$\frac{\partial P_j}{\partial t} = -\frac{\partial H}{\partial Q_j} = -\frac{\partial U}{\partial Q_j},$$

where  $j = 1-3N$ ,  $H$  is classical Hamiltonian,  $Q_j$  is Cartesian coordinate of  $j$ th mode and  $P_j$  is conjugated momentum. These equations were numerically solved by the Runge–Kutta method. No symmetry restriction was applied to the calculation of the energy gradients. The time step size was chosen as 0.10 fs, and a total of 5000 steps were calculated for each simulation. Sixteen snapshots of the trajectory at simulation time from 0.30 to 0.45 ps were sampled at every 50 fs interval and then hfcc is averaged for each temperature. The hfcc's of  $\text{H}_3\text{O}$  and  $\text{D}_3\text{O}$  at each point were calculated at the QCISD/6-311++G(3df,3dp) level of

theory. The drift of the total energy was confirmed to be  $< 0.1\%$  throughout at all steps in the trajectory. The momentum of the center of mass and the angular momentum around the center of mass were also confirmed to retain at the initial value of zero.

Static ab initio MO calculations were performed using GAUSSIAN 98 program package [19]. We carefully checked the effects of the basis sets and electron correlation on the calculated results [15]. By considering these effects, hfcc's of the  $\text{H}_3\text{O}$  and  $\text{D}_3\text{O}$  radicals were calculated by the QCISD/6-311++G(3df, 3dp) method at each selected point of the trajectory calculation. In all calculations, the expected values of  $\langle S^2 \rangle$  without spin annihilation were smaller than 0.7605.

### 3. Results

#### 3.1. Sample trajectories of $\text{D}_3\text{O}$ and $\text{H}_3\text{O}$ at 100 K

First, static ab initio MO calculations were carried out for the  $\text{H}_3\text{O}$  radical in order to evaluate the level of theory used in the present study. The structure of  $\text{H}_3\text{O}$  was fully optimized at the HF/6-311G(d, p) and QCISD/6-311++G(2df, 2dp) levels of theory. The optimized parameters are given in Table 1 together with hyperfine coupling constants (hfcc's) of the  $\text{H}_3\text{O}$  and  $\text{D}_3\text{O}$  radicals (see Fig. 1). The calculations showed that the  $\text{H}_3\text{O}$  radical has a bent form with bending angle (ca.  $112^\circ$ ). The hydrogen-, deuterium- and oxygen-hfcc calculated at the QCISD/6-311++G(3df, 3pd)/QCISD/6-311G(2df, 2dp) were  $a_{\text{H}} = 16.3$ ,  $a_{\text{D}} = 2.51$  and  $a_{\text{O}} = -207.4$  G, respectively. It should be noted that QCISD/6-311++G(3df, 3pd)/HF/6-311G(d, p) would give

reasonable values for hfcc's ( $a_{\text{H}} = 15.33$ ,  $a_{\text{D}} = 2.36$  and  $a_{\text{O}} = -206.3$  G) as shown in Table 1.

Ab initio MD calculations of  $\text{D}_3\text{O}$  and  $\text{H}_3\text{O}$  were carried out at temperatures 50, 100, 200, and 300 K. In this section, we will discuss the dynamics by using the results obtained for 100 K as a sample trajectory. The results of the trajectory calculations were given in Fig. 2. Solid and dotted curves are those for the  $\text{D}_3\text{O}$  and  $\text{H}_3\text{O}$  radicals, respectively.

The PE of the system of  $\text{D}_3\text{O}$  is plotted as a function of time in Fig. 2(a). PE vibrates with amplitude of 0.14 kcal/mol and period of 26 fs. Figs. 2(b) and (c) show the vibration of O–D distance and angle  $\phi$  plotted as a function of time, respectively. The amplitudes of O–D stretching and bending modes were calculated to be about 0.01 Å and  $6.9^\circ$ , respectively.

Fig. 2 also shows the result of the ab initio MD calculation of  $\text{H}_3\text{O}$  at 100 K (dotted lines). PE vibrates in the range 0.05–0.28 kcal/mol. The O–H distance is plotted in Fig. 2(b) as a function of time. The O–H distance is 1.0045 Å at time zero. The time period of the vibration was calculated to be 25 fs, and the distance is fluctuated in the range 1.0043–1.0098 Å, showing the amplitude of the O–H vibration is significantly small at 100 K. Fig. 2(c) shows umbrella bending mode of  $\text{H}_3\text{O}$  plotted as a function of time. The angle  $\phi$  vibrates in the range  $104.6$ – $111.0^\circ$ . Amplitudes of umbrella bending mode ( $\Delta\phi$ ) corresponding to the change of angle  $\phi$  for temperatures (50, 100, 200 and 300 K) were calculated to be  $\Delta\phi = 3.3^\circ$ ,  $6.4^\circ$ ,  $10.2^\circ$ , and  $12.7^\circ$ , respectively. Thus, the amplitude increases gradually with increasing temperature. These results mean that thermal energy activates mainly umbrella bending mode of  $\text{H}_3\text{O}$ .

Table 1

Optimized parameters of  $\text{H}_3\text{O}$ , total energies  $E$  (in a.u.), and hyperfine coupling constants hfcc's,  $a_{\text{H}}$ ,  $a_{\text{D}}$  and  $a_{\text{O}}$  (in gauss)

Method	$r$	$\theta$	$E$	$a_{\text{H}}$	$a_{\text{D}}$	$a_{\text{O}}$
HF/6-311G(d, p)	1.0045	111.56	–76.48082	21.73	3.34	–274.5
QCISD/6-311++G(2df, 2pd)	1.0123	112.01	–76.79489	16.34	2.51	–206.8
QCISD/6-311++G(3df, 3pd) <sup>a</sup>			–76.79906	16.30	2.51	–207.4
QCISD/6-311++G(3df, 3pd) <sup>b</sup>			–76.79893	15.33	2.36	–206.3

Bond lengths and angles are in Å and in degrees, respectively.

<sup>a</sup> Structure of  $\text{H}_3\text{O}$  was calculated at the QCISD/6-311++G(2df, 2pd) level.

<sup>b</sup> Structure of  $\text{H}_3\text{O}$  was calculated at the HF/6-311++G(d, p) level.

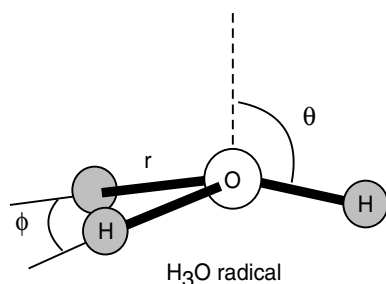


Fig. 1. Structure and geometrical parameters of the  $\text{H}_3\text{O}$  radical.

### 3.2. Time dependence of hfcc

The trajectory calculation was performed at each temperature in order to elucidate the finite temperature effects on the structure and hfcc's of the  $\text{H}_3\text{O}$  and  $\text{D}_3\text{O}$  radicals. Time dependence of hydrogen-, deuterium- and oxygen-hfcc of  $\text{H}_3\text{O}$  (H-, D- and O-hfcc) is given in Fig. 3. The H-hfcc's of three-hydrogen atoms are plotted as a function of time. H-hfcc of  $\text{H}_3\text{O}$  vibrates in the range 12–22 G at 100 K. Also, hfcc of the oxygen atom (O-hfcc) is fluctuated by temperature in the range –217 to –203 G. The averaged hfcc's for H and O atoms were calculated to be 15.92 and –208.10 G, respectively. As shown in Fig. 3(a), D-hfcc is significantly smaller than H-hfcc. The averaged hfcc of the D atom was 2.45 G.

### 3.3. Temperature dependence of hfcc's of $\text{H}_3\text{O}$ and $\text{D}_3\text{O}$

The H-, D- and O-hfcc of  $\text{H}_3\text{O}$  ( $\text{D}_3\text{O}$ ) calculated in the temperature range 0–300 K at the QCISD/6-311++G(3df,3pd) level are given in Table 2. Note that the H-, D- and O-hfcc at 0 K (denoted by  $a_{\text{H}}$ ,  $a_{\text{D}}$  and  $a_{\text{O}}$ ) were calculated by the static ab initio MO method. As shown in Table 2, H-hfcc increases with increasing temperature. For example, the value was calculated to be 16.73 G at 300 K, which is about 10% larger than that at 0 K (15.33 G). Thus, the H-hfcc of  $\text{H}_3\text{O}$  is largely affected by temperature, suggesting that the large shifts of H-hfcc might be observed by EPR experiment of  $\text{H}_3\text{O}$ . The D-hfcc of  $\text{D}_3\text{O}$  showed the similar tendency as that of H-hfcc of  $\text{H}_3\text{O}$ .

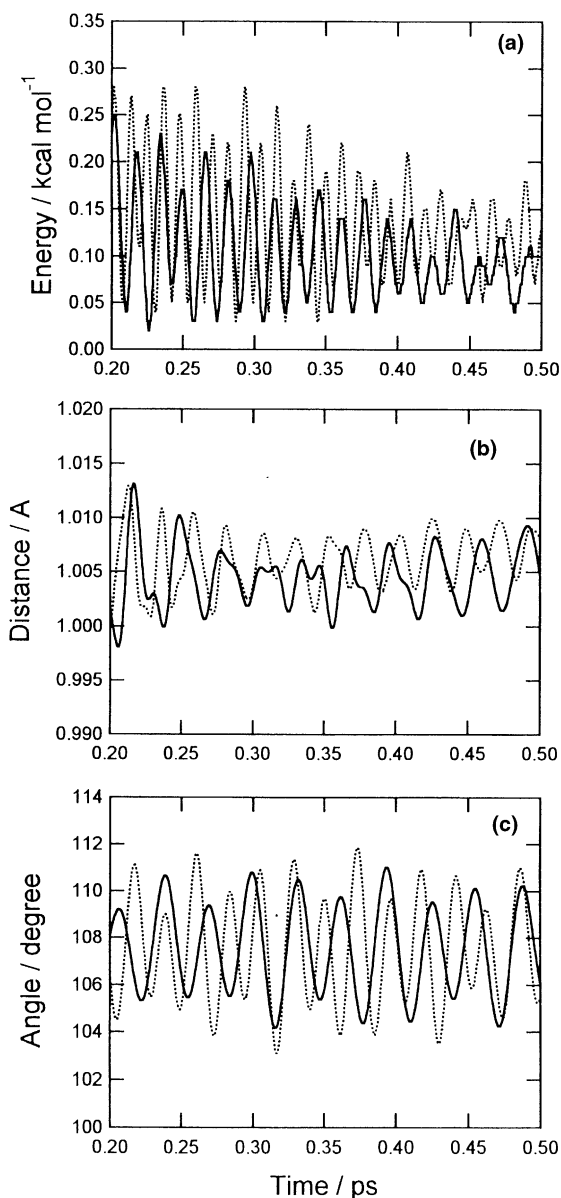


Fig. 2. Sample trajectories at 100 K for the  $\text{D}_3\text{O}$  radical (solid curve) and  $\text{H}_3\text{O}$  radical (dotted curve) plotted as a function of time: (a) PE of the system, (b) O–H (O–D) bond distance, and (c) angle  $\phi$  versus time.

### 4. Concluding remarks

In the present study, temperature effect on hfcc's of  $\text{H}_3\text{O}$  and  $\text{D}_3\text{O}$  was predicted on the basis of the full dimensional ab initio MD calculations.

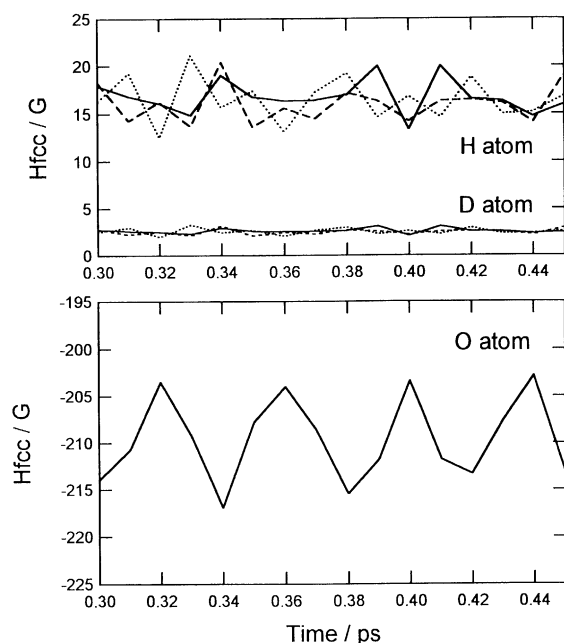


Fig. 3. H-, D- and O-hfcc (in G) calculated at the QCISD/6-311++G(3df,3dp) level plotted as a function of time.

Four temperatures (50, 100, 200, and 300 K) were examined in the calculations. From the MD calculations, it is predicted that D-hfcc of  $\text{D}_3\text{O}$  increases with increasing temperature. On the other hand, oxygen-hfcc decreases as temperature is increased.

Here, we will consider the origin of the temperature dependence of hfcc's of  $\text{H}_3\text{O}$  and  $\text{D}_3\text{O}$ . In a previous paper [15], we showed that H-hfcc of  $\text{H}_3\text{O}$  decreases as angle  $\theta$  is increased, whereas O-hfcc increases. For example, H- and O-hfcc at  $\theta = 90^\circ$  (planar structure) are calculated to be 33

and  $-261$  G, respectively. Also, it was indicated that the slope of PE curve calculated as a function of  $\theta$  is loose for small angle direction ( $90^\circ < \theta < 110^\circ$ ). On the other hand, that for larger angle direction ( $110^\circ < \theta$ ) is strongly steep [15]. Hence, the bending angle is more expanded to the small angle direction by thermal activation rather than the larger angle direction. This is the origin of temperature dependence of hfcc's of  $\text{H}_3\text{O}$ .

We have introduced several approximations to calculate the trajectories of  $\text{H}_3\text{O}$  and  $\text{D}_3\text{O}$ . First, we assumed that each atom of  $\text{H}_3\text{O}$  behaves as a classical particle on the full dimensional PE surface. The quantum effect was not considered in the present calculations. In particular, the zero point vibrational energy of the system was completely neglected. This effect might cause a slight change hfcc of  $\text{H}_3\text{O}$  at low temperature. Also, quantum mechanical tunneling effect was not considered in the trajectory calculations. There is a theoretical work about tunneling lifetime of  $\text{H}_3\text{O}$  radical in vacuo [11]. The estimated lifetimes of  $\text{H}_3\text{O}$  and  $\text{D}_3\text{O}$  are  $2 \times 10^{-13}$  and  $1 \times 10^{-12}$  s, respectively. This effect may increase the reaction probability for the dissociation of H atom from  $\text{H}_3\text{O}$  [2,11].

Second, HF/6-311G(d,p) multidimensional PE surface was employed in the trajectory calculations throughout. In a previous paper, we indicated that shape of PE surface of  $\text{H}_3\text{O}$  calculated at the HF/6-311G(d,p) level is in reasonably agreement with that of MP4SDQ calculation [2]. Hence, it is considered that the ab initio MD calculation at the HF/6-311G(d,p) level would give reasonable feature for the structure of  $\text{H}_3\text{O}$  at finite temperature. However, the dynamics calculation with more accurate wavefunction may provide deeper insight in the detailed dynamics feature of  $\text{H}_3\text{O}$ . Despite above approximations introduced here, the results enable us to obtain valuable information on the finite temperature effect on hfcc's of  $\text{H}_3\text{O}$ .

Table 2

Temperature dependence of time-averaged H-, D- and O-hfcc,  $a_{\text{H}}$ ,  $a_{\text{D}}$  and  $a_{\text{O}}$ , (in gauss) of  $\text{H}_3\text{O}$

Temperature (K)	$a_{\text{H}}$ (T)	$a_{\text{D}}$ (T)	$a_{\text{O}}$ (T)
0	15.33	2.36	-206.30
50	15.70	2.42	-207.45
100	15.92	2.45	-208.10
200	16.44	2.53	-209.60
300	16.73	2.57	-210.07

Values are calculated at the QCISD/6-311++G(3df,3pd) level of theory.

## Acknowledgements

The author is indebted to the Computer Center at the Institute for Molecular Science (IMS) for the use of the computing facilities. I also

acknowledge a partial support from a Grant-in-Aid from the Ministry of Education, Science, Sports and Culture of Japan.

## References

- [1] T.R. Geballe, T. Oka, *Nature* 384 (1996) 334.
- [2] H. Tachikawa, *Phys. Chem. Chem. Phys.* 2 (2000) 4327.
- [3] B.W. Williams, R.F. Porter, *J. Chem. Phys.* 73 (1980) 5598.
- [4] G.I. Gellene, R.F. Porter, *J. Chem. Phys.* 81 (1984) 5570.
- [5] R.E. March, A.B. Young, *Int. J. Mass Spectrom. Ion Processes* 85 (1988) 237.
- [6] H.J. Bernstein, *J. Am. Chem. Soc.* 85 (1963) 484.
- [7] T.W. Martin, L.L. Swift, *J. Am. Chem. Soc.* 93 (1971) 2788.
- [8] J.A. Wargon, F. Williams, *Chem. Phys. Lett.* 13 (1972) 579.
- [9] S. Noda, H. Yoshida, L. Kevan, *Chem. Phys. Lett.* 19 (1973) 240.
- [10] T.A. Claxton, I.S. Ginns, M.J. Godfrey, K.V.S. Rao, M.C.R. Simons, *J. Chem. Soc. Faraday Trans. II* 69 (1973) 217.
- [11] P.W. McLoughlin, G.I. Gellene, *J. Phys. Chem.* 96 (1992) 4396.
- [12] K.S.E. Niblaeus, B.O. Roos, P.E.M. Siegbahn, *Chem. Phys.* 25 (1977) 207.
- [13] D. Talbi, R.P. Saxon, *J. Chem. Phys.* 91 (1989) 2376.
- [14] A.E. Ketvirtis, J. Simons, *J. Phys. Chem.* 103 (1999) 6552.
- [15] H. Tachikawa, T. Yamano, *Chem. Phys. Lett.* 335 (2001) 305.
- [16] H. Tachikawa, *J. Phys. Chem. A* 105 (2001) 1260.
- [17] H. Tachikawa, *J. Phys. Chem. A* 104 (2000) 495.
- [18] H. Tachikawa, *J. Phys. Chem.* 192 (1998) 7065.
- [19] M.J. Frisch et al., *Ab initio MO program GAUSSIAN 98*, Revision A.5, Gaussian, Inc., Pittsburgh, PA, 1998.